J. Phycol. *, ***–*** (2016)

DOI: 10.1111/jpy.12395

PSEUDO-NITZSCHIA ARCTICA SP. NOV., A NEW COLD-WATER CRYPTIC *PSEUDO-NITZSCHIA* SPECIES WITHIN THE *P. PSEUDODELICATISSIMA* COMPLEX[1]

Isabella Percopo, Maria Valeria Ruggiero

Integrative Marine Ecology Department, Stazione Zoologica Anton Dohrn, Villa Comunale, Naples 80121, Italy

Sergio Balzano,[2] *Priscillia Gourvil*

Station Biologique, Sorbonne Universités, UPMC Univ Paris 06, CNRS, UMR 7144, Place Georges Teissier, Roscoff 29680, France

Nina Lundholm

The Natural History Museum of Denmark, University of Copenhagen, Sølvgade 83S, Copenhagen K 1307, Denmark

Raffaele Siano

DYNECO/Pelagos, IFREMER, Centre de Brest, BP 70, Plouzané 29280, France

Anna Tammilehto

The Natural History Museum of Denmark, University of Copenhagen, Sølvgade 83S, Copenhagen K 1307, Denmark

Daniel Vaulot

Station Biologique, Sorbonne Universités, UPMC Univ Paris 06, CNRS, UMR 7144, Place Georges Teissier, Roscoff 29680, France

and Diana Sarno[3]

Integrative Marine Ecology Department, Stazione Zoologica Anton Dohrn, Villa Comunale, Naples 80121, Italy

A new nontoxic *Pseudo-nitzschia* species belonging to the *P. pseudodelicatissima* complex, *P. arctica*, was isolated from different areas of the Arctic. The erection of *P. arctica* is mainly supported by molecular data, since the species shares identical ultrastructure with another species in the complex, *P. fryxelliana*, and represents a new case of crypticity within the genus. Despite their morphological similarity, the two species are not closely related in phylogenies based on LSU, ITS and *rbc*L. Interestingly, *P. arctica* is phylogenetically most closely related to *P. granii* and *P. subcurvata*, from which the species is, however, morphologically different. *P. granii* and *P. subcurvata* lack the central larger interspace which is one of the defining features of the *P. pseudodelicatissima* complex. The close genetic relationship between *P. arctica* and the two species *P. granii* and *P. subcurvata* is demonstrated by analysis of the secondary structure of ITS2 which revealed no compensatory base changes, two hemi-compensatory base changes, and two deletions in *P. arctica* with respect to the other two species. These findings emphasize that rates of morphological differentiation, molecular evolution and speciation are often incongruent for *Pseudo-nitzschia* species, resulting in a restricted phylogenetic value for taxonomic characters used to discriminate species. The description of a new cryptic species, widely distributed in the Arctic and potentially representing an endemic component of the Arctic diatom flora, reinforces the idea of the existence of noncosmopolitan *Pseudo-nitzschia* species and highlights the need for combined morphological and molecular analyses to assess the distributional patterns of phytoplankton species.

Key index words: **Arctic, cryptic, ITS; ITS2 secondary structure; LSU rRNA; morphology; *P. arctica* sp. nov.; phylogeny; *Pseudo-nitzschia*; *rbc*L**

***Abbreviations*: AIC, Akaike information criterion; ASP, amnesic shellfish poisoning; BIC, Bayesian information criterion; CBC, compensatory base change; DA, domoic acid; HCBC, hemi-compensatory base change; *rbc*S, Rubisco small subunit gene; SNP, single-nucleotide polymorphism**

Pseudo-nitzschia H. Peragallo is a worldwide genus of planktonic pennate diatoms, which includes a number of potentially toxic species. After the first ASP (amnesic shellfish poisoning) event in 1987 caused by the species *Pseudo-nitzschia multiseries* (Hasle) Hasle (Bates et al. 1989), numerous studies have focused on several aspects of taxonomy, ecology,

[1]Received 29 July 2015. Accepted 17 December 2015.
[2]Present address: Department of Marine Organic Biogeochemistry, Nioz Royal Netherlands Institute for Sea Research, P.O. Box 59, 1790 Ab Den Burg, Texel, the Netherlands.
[3]Author for correspondence: e-mail diana.sarno@szn.it.
Editorial Responsibility: T. Mock (Associate Editor)

toxicity, and physiology of *Pseudo-nitzschia* species (Lelong et al. 2012, Trainer et al. 2012). The increased interest in *Pseudo-nitzschia* biodiversity and distribution clearly resulted in a steady increase in the number of species descriptions (Lelong et al. 2012). Most of the diversity has been discovered within the *P. pseudodelicatissima* complex. The *P. pseudodelicatissima* complex was introduced in 2003 when Lundholm and coauthors emended the species *P. pseudodelicatissima* (Hasle) Hasle and *P. cuspidata* (Hasle) Hasle, and described two similar species *P. caciantha* Lundholm, Moestrup and Hasle and *P. calliantha* Lundholm, Moestrup and Hasle based on morphological and molecular (LSU and ITS) data (Lundholm et al. 2003). Since this first study, different genetic markers have been used for molecular taxonomy of *Pseudo-nitzschia* spp., including the mitochondrion encoded cytochrome c oxidase 1 (*cox*1; Kaczmarska et al. 2008), the chloroplast-encoded genes of the large subunit of ribulose-1,5-bisphosphate carboxylase/oxygenase (*rbc*L; Amato et al. 2007, Casteleyn et al. 2009, 2010) and of the small subunit (*rbc*S; Delaney et al. 2011). However, the internal transcribed spacer (ITS) of the nuclear ribosomal operon was shown to be the best species discriminator among all tested genetic markers for *Pseudo-nitzschia* species (Lundholm et al. 2003, Amato et al. 2007, Casteleyn et al. 2008, Kaczmarska et al. 2008). Information contained in the second internal transcribed spacer (ITS2) has been useful to help the delimitation of some cryptic/pseudo-cryptic species (e.g., *P. mannii* Amato and Montresor, *P. arenysensis* Quijano-Scheggia, Garcés, Lundholm, *P. hasleana* Lundholm and *P. fryxelliana* Lundholm; Amato and Montresor 2008, Quijano-Scheggia et al. 2009, Lundholm et al. 2012). Currently, the *P. pseudodelicatissima* complex alone includes 16 species (Lundholm et al. 2003, Amato et al. 2007, Amato and Montresor 2008, Lim et al. 2012, 2013, Orive et al. 2013, Teng et al. 2014).

The genus *Pseudo-nitzschia* is known to be distributed worldwide but species biogeography and local phenologies are far from being assessed exhaustively (Hasle 2002). Microscopic observations have suggested that some species seem to be restricted to distinct latitudinal zones. This is particularly evident for a number of cold-water species, as is the case of *P. turgiduloides* (Hasle) Hasle and *P. subcurvata* (Hasle) Fryxell found in the Antarctic waters (Hasle and Syvertsen 1997, Scott and Thomas 2005), or *P. granii* (Hasle) Hasle recorded in arctic and subarctic waters (Lovejoy et al. 2002, Marchetti et al. 2008). In Arctic waters, in addition to *P. granii*, other *Pseudo-nitzschia* species have been recorded in sea ice, coastal (Poulin et al. 2011) and offshore waters (Marchetti et al. 2008). In particular, six taxa have been recorded in the arctic waters of Alaska, Canada and Greenland: *P. pseudodelicatissima* and *P. pungens* (Grunow ex Cleve) Hasle from Chucky and Beaufort Sea (Booth and Horner 1997, Różańska et al. 2008, Sukhanova et al. 2009), *P. obtusa* (Hasle) Hasle and Lundholm from Chucky Sea (Booth and Horner 1997), *P. delicatissima* (Cleve) Heiden, *P. seriata* (Cleve) H. Peragallo and *P. granii* from Baffin Bay and Greenland (Lovejoy et al. 2002, Hansen et al. 2011, Hardardotir et al. 2015). A higher number of species have been reported from the Russian Arctic (Tuschling et al. 2000) and Scandinavia (von Quillfeldt 1997, 2000, Ratkova et al. 1998, Wassmann et al. 1999, Ratkova and Wassmann 2002, 2005, Degerlund and Eilertsen 2010). However, information on species occurrence in Arctic waters is generally based on morphological observations acquired using light microscopy (LM). Given the existence of high level of cryptic diversity within the genus, and the evidence that, even at a regional scale, several distinct genetic lineages can coexist and have different seasonality (McDonald et al. 2007, Orive et al. 2013, Ruggiero et al. 2015), the biogeography and distribution of cold temperature *Pseudo-nitzschia* species needs to be re-evaluated.

In this study, we investigate ultrastructure, molecular and toxicity characteristics of six strains of *Pseudo-nitzschia*, isolated from different regions of the Arctic. One of the isolated strains (P2F2) was previously identified as *P. delicatissima* (Tammilehto et al. 2012) and the other (CCMP1309 = K1142) as *P.* cf. *subcurvata*. Detailed morphological analyses and the use of discriminating genetic markers (LSU, *rbc*L, and ITS, including secondary structure) suggest that all mentioned strains belong to a new species, that we describe as *P. arctica* sp. nov.

MATERIAL AND METHODS

Samples and cultures. A total of six strains of *P. arctica* were analyzed (Table 1). Four strains were isolated from seawater collected in the Beaufort Sea, at 29 m in a station located near the Mackenzie River outlet, in the framework of the MALINA cruise which took place in mid-summer 2009. Clonal strains were obtained through single-cell pipette isolation after seawater enrichment. The media used for the enrichments were 2-fold diluted Keller medium (K/2, Keller et al. 1987) for RCC2517 and RCC2002 and Javorski medium (www.ccap.ac.uk/media/recipes/JM.htm) for RCC2004 and RCC2005. The media were adjusted to a salinity of 30. Both types of enrichments were maintained at 4°C, in 12:12 light:dark conditions under an irradiance of 10–20 μmol photons $\cdot$ m^{-2} $\cdot$ s^{-1} for 3–4 months before strains isolation. Single-cell pipette isolations were carried out as described previously (Balzano et al. 2012a): samples were observed using an inverted microscope Olympus IX71 (Olympus, Hamburg, Germany) and 1.5 mL from each sample were collected and transferred into a 24-well Iwaki plate (Starlab, Bagnieux, France). A sample aliquot was transferred into a new well containing sterile medium and this step was repeated 4 times for a final 100,000-fold dilution of the enriched sample. Single cells were then collected using a Nichipet EX 0.5–10 μL (Starlab), transferred again into new plates containing sterile media and incubated in the same conditions as the enrichment. These cultures are currently (November 2015) available from the Roscoff Culture Collection (http://www.roscoff-culture-collection.org/). They are maintained in K/2 plus Si medium. One other strain (P2F2) was established

TABLE 1. Strain designation, isolation site and date, and accession numbers for cultures of *Pseudo-nitzschia* established for this study.

Species	Strain designation	Isolation site	Station coordinates Latitude [°N]–Longitude [°W]	Collection date	Accession number (LSU)	Accession number (ITS)	Accession number (*rbc*L)
P. arctica	RCC2002	Beaufort Sea	69.49–137.94	August 2009	JQ995416	KT808253	KT808257
P. arctica	RCC2004	Beaufort Sea	69.49–137.94	August 2009	JQ995418	KT808254	As KT808257
P. arctica	RCC2005	Beaufort Sea	69.49–137.94	August 2009	JQ995419	KT808255	KT808258
P. arctica	RCC2517	Beaufort Sea	69.49–137.94	August 2010	JQ995461	KT808256	KP757864
P. arctica	P2F2	Disko Bay, West Greenland	69.14–53.23	April 2010	KU212806	KT589421	
P. arctica	CCMP1309 = syn K1142	Barrow Strait, Baffin Bay	74.66–95.16	May 1989	As KU212806	AY556482	

from field sample in Disko Bay, Greenland, in April 2010, using single-cell isolation techniques. The strain CCMP1309 was isolated from a sample in Barrow Strait, Canada in May 1989 and is available from the NCMA collection (https://ncma.bigelow.org/ccmp1309) where it is identified as *P.* cf. *subcurvata*. The latter two strains were grown at 4°C in L1-medium (Guillard and Morton 2003), at a salinity of 30 under a light intensity of 100 µmol photons · m^{-2} · s^{-1} at a 15:9 light:dark cycle using cool white fluorescent bulbs.

Microscopy. LM observations and measurements of live cells were carried out using a Zeiss Axiophot light microscope (Carl Zeiss, Oberkochen, Germany) equipped with Nomarski differential interference contrast (DIC), phase contrast (PH) and bright-field (BF) optics. Cell end overlap was measured in colonies observed in girdle view and the percentage of overlap calculated. Pictures were taken with a Zeiss Axiocam digital camera (Carl Zeiss). For transmission electron microscopy (TEM) observations, some samples were treated with nitric and sulfuric acids (1:1:4, sample:HNO_3:H_2SO_4), boiled for some seconds to remove the organic matter and washed with distilled water (modified from Round et al. 1990). Other samples were treated according to Lundholm et al. (2002). Acid-cleaned material was mounted on Formvar-coated grids. All grids were observed either using a Philips 400 TEM (Philips Electron Optics BV, Eindhoven, the Netherlands) or a JEOL-1010 TEM (Jeol, Tokyo, Japan). Morphometric measurements were taken on TEM images. Approximately, 20 valves of each strain were observed.

Molecular analysis. DNA extraction: For DNA extraction, 2 mL of culture were collected during the stationary growth phase, centrifuged at 12,800*g* for 10 min and 1.8 mL supernatant removed. For strains RCC2002, RCC2004, RCC2005, and RCC2517, genomic DNA was then extracted from the pellets using Qiagen Blood and Tissue kit (Qiagen, Cortaboeuf, France) as described previously (Balzano et al. 2012b). For strains P2F2 and CCMP1309, genomic DNA was extracted as in Lundholm et al. (2002).

PCR amplification: DNA from each strain was amplified by PCR for the genes of LSU rRNA, ITS1-5.8S-ITS2 and *rbc*L. For all PCR reactions, 1 µL of genomic DNA was mixed with 0.5 µL of 10 µM solution of both forward and reverse primers, 15 µL of HotStar Taq Plus Master Mix Kit (Qiagen), 3 µL of Coral Load (Qiagen), and Milli-Q water up to a final volume of 30 µL.

The LSU rRNA gene was amplified and sequenced using primers D1R or D3Ca targeting the D1-D3 region of the nuclear LSU rRNA (Orsini et al. 2002). The ITS region of the rRNA operon was amplified and sequenced using the universal primers ITS-1 and ITS-4 which amplify very small portions of both 18S and LSU rRNA genes and the whole ITS region (White et al. 1990).

The *rbc*L gene was amplified using primers *rbc*L1 and *rbc*L7 (Amato et al. 2007) and PCR reactions included an initial denaturation of 94°C for 5 min, 35 amplification cycles (94°C for 60 s, 60°C for 55 s, and 72°C for 90 s) and a final extension of 5 min at 72°C (see Table S1 in the Supporting Information for primer sequences).

PCR amplicons were purified using exosap (USB Products, Santa Clara, CA, USA) and sequences were determined using the Big Dye Terminator V3.1 (Applied Biosystems, Foster City, CA, USA). For sequencing, two additional internal primers, *rbc*LI1F and *rbc*LI1R, were used (Amato et al. 2007) along with the primers described above.

Chromatograms of the sequences obtained were then analyzed by eye to check for the presence of double peaks and nucleotide ambiguities using Bioedit (Hall 1999).

Molecular phylogenies: *Pseudo-nitzschia* sequences obtained from GenBank for each marker (ITS, LSU and *rbc*L) were aligned with sequences of our strains using MAFFT (Katoh 2013) (Table S2 in the Supporting Information), with the Q-INS-i options, which incorporates structural information. The LSU rRNA alignment (55 sequences) included 943 bp, of which 242 positions were analyzed (26%), after eliminating all positions containing gaps and missing data. *Cylindrotheca fusiformis* Reimann and Lewin was used as outgroup. The ITS rRNA (58 sequences) alignment included initially 1401 positions, of which, after eliminating all positions containing gaps and missing data, 609 positions were analyzed (44%). The ITS analyses were unrooted. The *rbc*L alignment (35 sequences) included 1,509 bp of which 1378 positions were analyzed (91%), after eliminating all positions containing gaps and missing data. *Cylindrotheca* sp. was used as outgroup. Sequences of *P. subcurvata* (Accession number: HQ337586 and HQ337585) were too short (748 over 1,509 bp of alignment) to be included in the phylogenetic *rbc*L analysis but they were used to estimate the diversity between species using number of net nucleotide substitutions per site between species (Nei 1987). All distance and maximum likelihood analyses were performed in MEGA v5.10 (Tamura et al. 2011). Maximum Likelihood trees were built using MEGA v5.10, with 1,000 bootstrap replicates, based on the substitution model selected through the Akaike information criterion option implemented in MEGA v5.10. Bayesian analyses were performed using MrBayes 3.1.2 (Ronquist and Huelsenbeck

2003), with four chains run for 1,000,000 generations. The temperature was set to 0.2, sample frequency was 100, and the number of burn-in generations was 25% for each data set. Bayesian Inference was performed with the best model selected through the Bayesian information criterion implemented in MEGA v5.10. The number of net nucleotide substitutions per site between species (Nei 1987) was assessed for each marker using the software DNAsp (Librado and Rozas 2009).

Secondary structure of ITS2. The secondary structure of the ITS-2 from *P. arctica* strain RCC2005 was predicted using mfold (http://unafold.rna.albany.edu, Zuker et al. 1999) using the default parameters: 37°C, 1 M sodium chloride, 5% sub-optimality and maximum loop sizes of 30 bp. The secondary structure showing the typical folding of the genus *Pseudo-nitzschia* (i.e., four helices and one pseudohelix) and the lowest free energy (dG = −81.40) was selected and data were downloaded in dot-bracket notation. The structure of *P. granii* strain RCC2008 and *P. subcurvata* 1-F was then reconstructed using the ITS2 database (http://its2.bioapps.biozentrum.uni-wuerzburg.de, Wolf et al. 2005) by homology modeling using the secondary structure of *P. arctica* as template. The secondary structures were then visualized and downloaded using VARNA (Darty et al. 2009) to identify compensatory base changes (CBCs) and hemi-compensatory base changes (HCBCs).

Toxin analysis. Domoic acid (DA) production of strains RCC2002, RCC2004, RCC2005 was screened by an Elisa test kit (Mercury Science, Inc., Durham, NC, USA). Toxicity tests were carried out on late-stationary phase cultures on material harvested from 50 mL culture maintained in the standard maintenance conditions (K/2 plus Si medium, 4°C, 70–80 µmol photons $\cdot$ m^{-2} $\cdot$ s^{-1}, 12:12 light:dark regime). Culture material was sonicated and then filtered onto GF/F filters. Assays were performed following manufacturer's specifications, using a standard microplate absorbance reader at 450 nm. The assay test used had a limit of detection 0.1 µg DA $\cdot$ L^{-1}. However, Elisa test might be considered as qualitative tests for general screening of DA production. Toxin production of strain P2F2 was tested under two different conditions (see details in Tammilehto et al. 2012): (i) using 50% silica-reduced L1-medium, under a light intensity of 100 µmol photons $\cdot$ m^{-2} $\cdot$ s^{-1} using 19:5 light:dark cycle. The silica concentration of the L1-medium was reduced in order to trigger DA production as Si-limitation is known to enhance DA production in *Pseudo-nitzschia* species (e.g., Fehling et al. 2004); (ii) under similar conditions and in addition exposed to grazing copepods of the genus *Calanus*, as this is known to induce DA production (Tammilehto et al. 2012, 2015, Hardardotir et al. 2015). Processing of the material and toxin analyses using Liquid Chromatography–Mass Spectrometry (LC MS/MS) is described in Tammilehto et al. (2012).

RESULTS

Diagnosis. ***Pseudo-nitzschia arctica*** Percopo et Sarno **sp. nov**. (Fig. 1, A–J; Table 2)

Cells are lanceolate in valve view, linear in girdle view forming stepped colonies with about 1/9–1/12 of cell overlapping. Transapical axis length is 1.6–2.5 µm. Central larger interspace is present. Fibulae are not always regularly spaced. 17 to 24 fibulae and 33 to 39 interstriae in 10 µm. Each stria has one row of rounded poroids. 4 to 6 poroids in 1 µm. Each poroid contains 1–5 sectors or consists of less silicified unperforated areas. The cingulum is composed of three open bands. The valvocopula has 41–48 striae in 10 µm and is 1–3 poroids high and two poroids wide. The second band is one poroid high and 1–2 poroids wide. The second band is split in two parts: one with small variable poroids and the other completely unperforated. The third band is generally unperforated.

Holotype: Slide of the strain RCC2005 deposited at the Museum of the Stazione Zoologica A. Dohrn in Napoli, registered as no. SZN-RCC2005/1.

Isotype: Fixed material of RCC2005 deposited at the Museum of the Stazione Zoologica A. Dohrn in Napoli, registered as no. SZN-RCC2005/2.

Illustrations of the type material: Figure 1, F, H and J.

Molecular characterization: DNA sequences for rRNA LSU, ITS and *rbc*L of strain RCC2005 are deposited in GenBank with accessions number JQ995419, KT808255 and KT808258, respectively.

Type locality: Beaufort Sea, 69.49°N, 137.94°W

Etymology: The epithet *arctica* (=arctic) refers to the area where the organism was found.

Morphology: Cells are lanceolate in valve view and almost linear with truncated ends in girdle view (Fig. 1, A and B). Cells overlap about 1/9–1/12 of total cell length when forming stepped colonies (Fig. 1A). Valvar transapical axis length is 1.6–2.5 µm, apical axis 26–67 µm (Table 2). Valves are tapering toward the ends with rounded apices (Fig. 1, B–D). A central larger interspace is present (Fig. 1, E and G). The fibulae are not always regularly spaced. The densities of fibulae and interstriae are 17–24 and 33–39 in 10 µm, respectively. Each stria contains one row of rounded poroids with a density of 4–6 poroids in 1 µm (Fig. 1, E–I; Table 2). The mantle is often 1–2 poroids high and has a composition similar to the valve (Fig. 1F). Each poroid contains 1–5 sectors of varying size and lacks a central sector. The most frequent number of sectors in the examined strains is 1–3 (Fig. 1, E–I). In some cases, the poroids simply consist of less silicified areas without any perforation (Fig. 1, E–I). The cingulum is composed of three open bands (Fig. 1, F and J–L). The valvocopula contains 41–48 striae in 10 µm and is 2 and seldom 1 or 3 poroids high and 2 poroids wide (Fig. 1, J–L; Table 2). The second band contains a longitudinal row of variable size poroids and an unperforated part (Fig. 1, J and L). The third band is generally unperforated and has rarely a few scattered minute pores (Fig. 1J). A certain variability was observed among the different strains of *P. arctica*; in particular, the strain RCC2004 has poroids with a higher number of dividing sectors (up to 5) with a central sector rarely present (Fig. 1G), and in the strain P2F2 the valvocopula tends to be slightly more silicified and 3 instead of 2 poroids high, the second band has more defined and larger poroids and the third band is often perforated by minute pores (Fig. 1K).

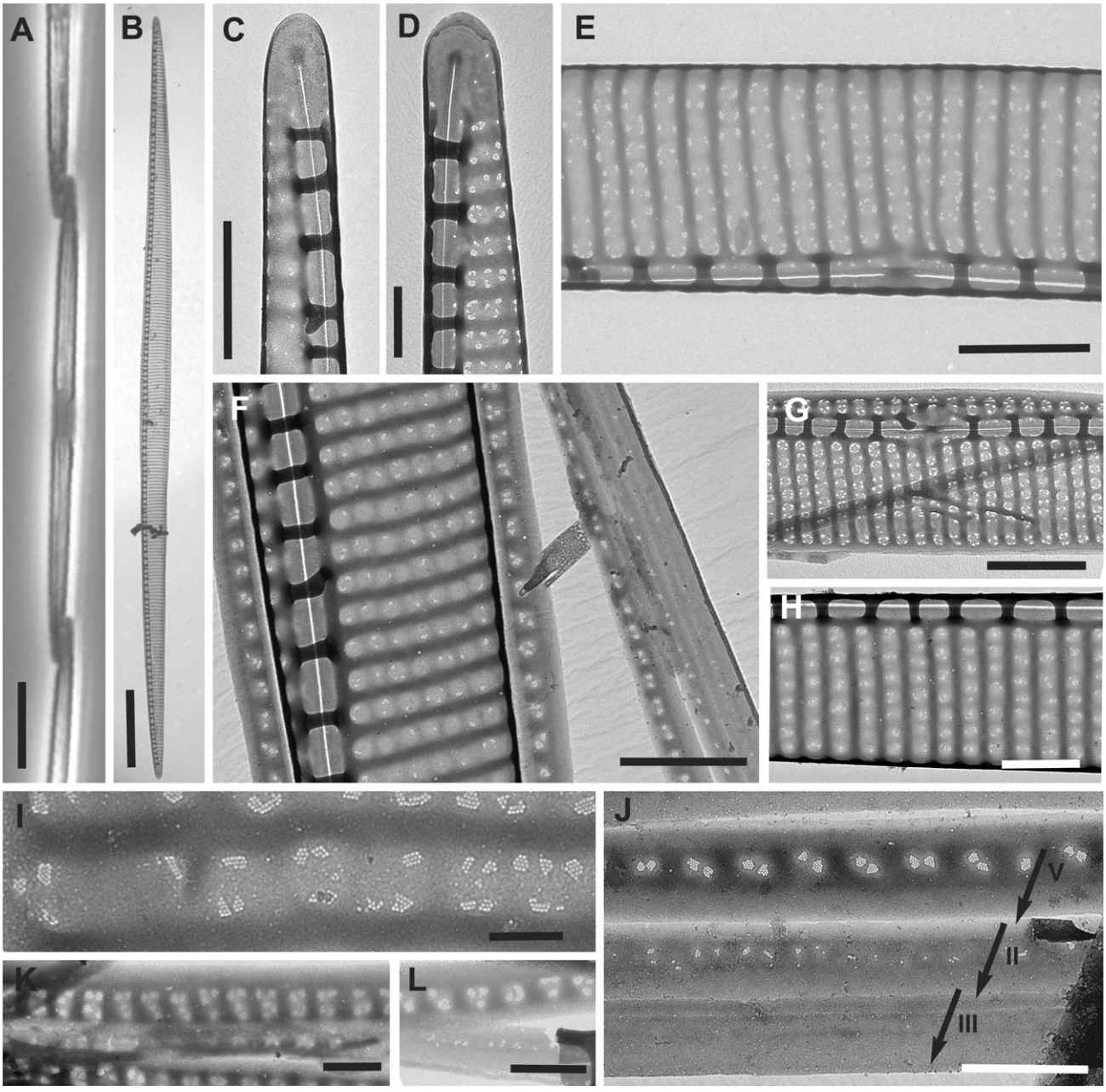

FIG. 1. LM (A) and TEM micrographs (B–I) of *Pseudo-nitzschia arctica* sp. nov. (A) Strain RCC2004. Part of a colony in girdle view. (B) Strain P2F2. Whole cell. (C and D) Strain RCC2004. Valve ends. (E) Strain P2F2. Central part of the valve with central nodule. (F) Strain RCC2005. Part of valve with mantle and cingular bands. (G) Strain RCC2004. Central part of the valve showing stria structure. Note the well-formed poroids. (H) Strain RCC2005. Part of valve with poroids with less silicified areas. (I) Strain P2F2. Particular of poroid structure. Note missing poroids and sectors. (J) Strain RCC2005. The three cingular bands. Arrows indicate borders of bands: V = valvocopula, II = second cingular band, III = third cingular band. (K) Strain P2F2. Valvocopula and second cingular band. (L) Strain P2F2. Second and third cingular bands with small pores. Scale bars: (A) = 10 μm, (B) = 5 μm, (C, E, F, G, H) = 1 μm, (D, J, K, L) = 0.5 μm, (I) = 0.2 μm.

Toxicity. Toxicity tests on *P. arctica* strains for DA production were negative for both ELISA tests (strains RCC2002, RCC2004, RCC2005) and LC MS/MS analyses (strain P2F2).

Phylogenetic analysis. Phylogenies based on LSU (Fig. S1 in the Supporting Information), ITS and ITS2 (Fig. 2 and Fig. S2 in the Supporting Information), and *rbc*L (Fig. 3) showed *P. arctica* strains clustering together in a well-supported clade (LSU: 99/100, ITS: 99/1.00, ITS2: 99/1.00, *rbc*L: 100/1.00, bootstrap and Bayesian values, respectively), as sister to a clade comprising *P. granii* and *P. subcurvata.* LSU, ITS, and *rbc*L sequences were identical for all strains of *P. arctica* (although the *rbc*L sequence for

TABLE 2. Morphometric data of *P. arctica* compared to species of the *P. pseudodelicatissima* complex and *P. granii* and *P. subcurvata*.

		Valves						Poroids		Intercalary bands	
Species	Reference	Valve shape	Width (μm)	Length (μm)	Fibulae in 10 μm	Central nodule	Interstriae in 10 μm	Poroids in 1 μm	Sectors in poroids	Band striae in 10 μm	Valvocopula striae: poroids wide x poroids high
P. arctica	This study	Lanceolate	1.6–2.5 1.9 ± 0.2 (*n* = 61)	26–67 53.7 ± 13.4 (*n* = 20)	17–24 20.4 ± 1.7 (*n* = 100)	+	33–39 35.9 ± 1.5 (*n* = 106)	4–6 5.5 ± 0.5 (*n* = 106)	0–5 var.	41–48 44.3 ± 2.0 (*n* = 63)	2 × 1–3
P. abrensis	Orive et al. (2013)	Linear to lanceolate	1.7–2.5 2.0 ± 0.2	66.5–74.1	16–22 18.6 ± 1.3	+	30–37 32.8 ± 2.0	4–6 5.2 ± 0.4	1–4 2.3 ± 0.5	36–38 36.8 ± 0.8	2 × 2–4
P. batesiana	Lim et al. (2013)	Lanceolate	1.8–2.2 2.0 ± 0.2	84–86 84.8 ± 1.0	15–19 17.0 ± 2.0	+	29–32 30.6 ± 1.6	5–6 5.5 ± 0.5	2–3 2.6 ± 0.6	40–43 41.3 ± 1.5	2 × 3–4
P. caciantha	Lundholm et al. (2003)	Lanceolate	2.7–3.5	53–75	15–19	+	28–31	3.5–5	4–5	33–38	2 × 3–5
	Amato et al. (2007)	Lanceolate	2.2–3.0 2.6 ± 0.2	nd	18–23 20.7 ± 1.5	+	33–37 34.9 ± 1.5	3–5 4.6 ± 0.1	2–6 3.1 ± 1.0	nd	nd
P. calliantha	Lundholm et al. (2003)	Linear	1.4–1.8	41–98	15–22	+	34–39	4–6	7–10	42–48	2–3 × var.
	Lundholm et al. (2012)	Linear	1.3–1.8 1.6 ± 0.2	nd	18–24 20.3 ± 1.6	+	35–41 38.0 ± 2.0	4–5 4.9 ± 0.4	7–10 8.5 ± 1.0	42–50 46.6 ± 2.5	2–3 × var.
P. circumpora	Lim et al. 2012	Lanceolate	2.2–2.7 2.5 ± 0.3	70.9–88.2 79.5 ± 8.7	15–19 17.1 ± 2.0	+	32–35 33.7 ± 1.7	1–4 2.9 ± 1.3	>7	40–42	2 × 4
P. cuspidata	Lundholm et al. (2003)	Lanceolate	1.4–2.0	30–73	19–25	+	35–44	4–6	2	47–53	Split poroids
P. fryxelliana	Lundholm et al. (2012)	Lanceolate	2.1–2.5 2.2 ± 0.2	30–54 37.6 ± 8.7	(17) 18–25 20.6 ± 1.9	+	34–40 36.7 ± 1.4	5–6 (7) 5.7 ± 0.5	(1) 2–3 2.3 ± 0.6	41–50 44.1 ± 2.3	2 × 1–3
P. fukuyoi	Lim et al. (2013)	Linear to lanceolate	1.5–1.9 1.7 ± 0.2	74–81 77.2 ± 3.3	17–19 17.8 ± 1.0	+	32–34 33.0 ± 1.3	5–6 5.1 ± 0.5	2–3 (4) 2.4 ± 0.8	39–47 42.9 ± 3.8	2 × 3–4
P. hasleana	Lundholm et al. (2012)	Lanceolate	1.5–2.8 2.0 ± 0.4	37–79 53.3 ± 11.2	13–20 16.3 ± 1.6	+	31–40 35.4 ± 2.1	5–6 5.3 ± 0.5	2–6 3.6 ± 1.2	37–46 (47) 42.4 ± 2.3	2 × 3–6
P. inflatula	Hasle (1965)	Linear-lanceolate/ inflated	1.5–2.5	60–100	18–21	+	32–35	5	2	nd	nd
	Priisholm et al. (2002)	Linear/inflated	1.3–1.8	55–75	21–30	+	38–46	6–8	1–3	46–52	nd
P. kodamae	Teng et al. (2014)	Linear	2.1–3.3	50.8–86.2	12–16	+	22–29	3–5	2–4 (5)	33–36	2 × 2–3
P. lineola	Lundholm et al. (2012)	Linear-lanceolate	2.0–2.8 2.4 ± 0.2	71–95 83.2 ± 5.9	10.5–15.5 13.2 ± 1.0	+	22–31 25.0 ± 2.4	3–6 4.3 ± 0.7	1–2 rows poroids	22–34 25.4 ± 2.8	2–3 × 2–3
	Cleve (1897)	Linear-lanceolate	2	100–110	14	+	24	nd	nd	nd	nd
	Hasle (1965)	Linear-lanceolate	1.8–2.7	56–112	11–16	+	22–28	3–7	1–2 rows poroids	nd	nd
P. lundholmiae	Lim et al. (2013)	Lanceolate	1.7–2.3 2.0 ± 0.3	63–73 68.1 ± 4.8	16–18 17.0 ± 1.1	+	28–34 30.7 ± 2.9	4–6 5.2 ± 0.8	1–2 (3) 1.8 ± 0.5	35–40 37.6 ± 2.5	1–2 × 2–3
P. mannii	Amato and Montresor (2008)	Linear	1.7–2.6 2.1 ± 0.2	33–130	17–25 20.2 ± 2.0	+	30–40 35.8 ± 2.1	4–6 4.8 ± 0.3	2–7 3.5 ± 1.0	47	2 × 3–4

(continued)

TABLE 2. (continued)

		Valves						Poroids		Intercalary bands	
Species	Reference	Valve shape	Width (μm)	Length (μm)	Fibulae in 10 μm	Central nodule	Interstriae in 10 μm	Poroids in 1 μm	Sectors in poroids	Band striae in 10 μm	Valvocopula striae: poroids wide x poroids high
P. plurisecta	Orive et al. (2013)	Linear to lanceolate	1.5–2.0 1.7 ± 0.1	56.3–59.7	17–25 20.7 ± 1.7	+	34–45 37.3 ± 2.3	4–7 5.6 ± 0.6	3–10 5.5 ± 1.5	45–48.5 47.2 ± 1.3	2 × 3–5
P. pseudodelicatissima	Lundholm et al. (2003)	Linear	0.9–1.6	54–87	20–25	+	36–43	5–6	2	48–55	Split poroids
	Amato et al. (2007)	nd	1.5–1.9 1.8 ± 0.1	nd	20–29 23.5 ± 1.8	+	34–45 41.8 ± 1.9	4–7 5.6 ± 0.6	2	nd	nd
P. granii	Hasle and Syvertsen (1997)	Linear/spindle	1.5–2.5	25–79	12–18	–	44–49	nd	nd	nd	nd
	Marchetti et al. (2008)	Linear/spindle	1.4–1.9	21–88	12–20	–	49–55	6–7	4–6[a]	nd	nd
P. subcurvata	Hasle and Syvertsen (1997)	Curved	1.5–2.5	47–113	12–18	–	44–49	nd	5–6[b]	nd	nd
	Almandoz et al. (2008)	Curved	1.3–1.8	48–86	12–22	–	43–55	6–8	nd	nd	nd

[a]Not in the text but inferred from plate 13, fig. 7a, in Hasle 1964, and fig. 2, in Marchetti et al. 2008.
[b]Not in the text but inferred from plate 13, figs. 2a and 4, in Hasle 1964.
Data are given as minimum and maximum range (above), and mean value ± SD (below). nd, no data; var, variable.

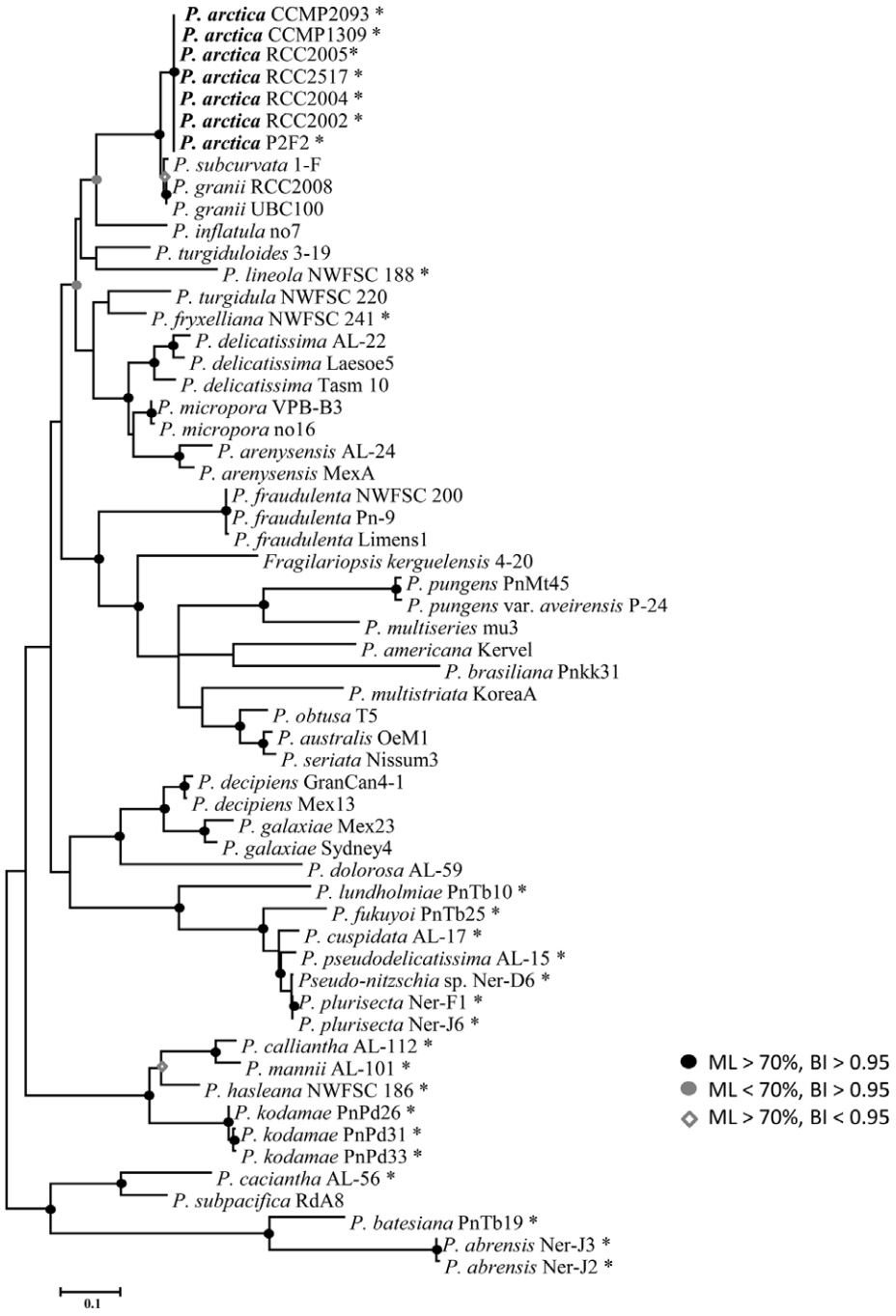

FIG. 2. Phylogenetic tree from maximum likelihood (ML) analysis based on *Pseudo-nitzschia* ITS1-5.8S-ITS2 region of the ribosomal RNA. The tree is unrooted. Black circle indicates boostrap support and bayesian posterior probabilities on >70% and 95%, respectively; gray circle indicates boostrap support below 70% and bayesian posterior probabilities on 95%; gray diamond indicates boostrap support on 70% and bayesian posterior probabilities below 95%. * indicate the species belonging to the *P. pseudodelicatissima* complex.

P2F2 and CCMP1309 were not available). Notably, ITS GenBank sequences of CCMP2093 isolated from the arctic Nunavut, Canada, originally assigned to *P.* cf. *granii*, is identical to *P. arctica* ITS sequences, and should be reassigned to *P. arctica*.

Genetic distances between *P. arctica* and its closest relatives, *P. granii* and *P. subcurvata* were small for all markers. *P. granii* and *P. subcurvata* were more closely related to each other than to *P. arctica*. Divergence values were variable among different genetic markers when comparing *P. arctica* with the other two closely related species, with LSU showing the lowest values and *rbc*L the highest (Table 3).

Secondary structure of ITS2. ITS2 secondary structure of *P. arctica* presented the typical folding with four helices plus the additional helix IIa, characteristic of the genus *Pseudo-nitzschia* (Fig. 4). Secondary structures were compared among *P. arctica* and its sister species *P. granii* and *P. subcurvata*. No CBCs, two HCBCs and four SNPs (single-nucleotide polymorphisms) were observed between *P. arctica* and the closely related species *P. granii* and *P. subcur-*

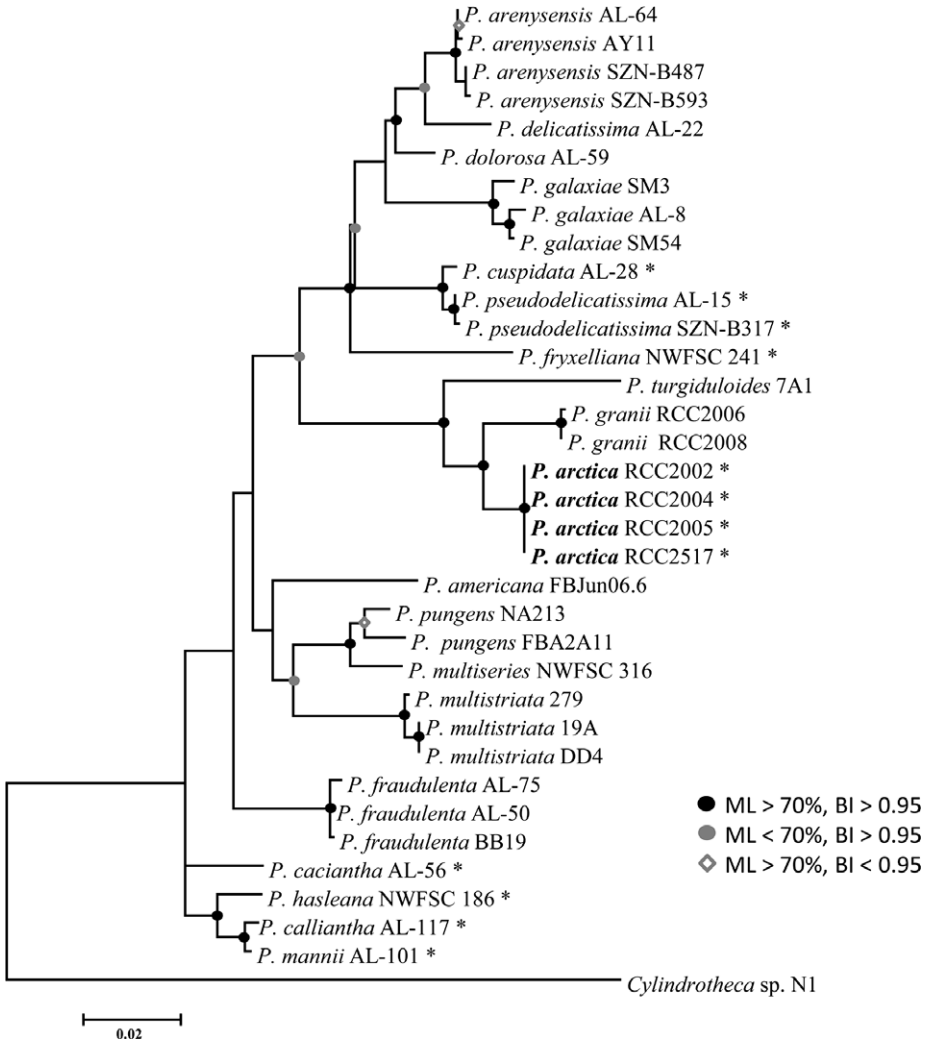

FIG. 3. Phylogenetic tree from ML analysis based on *Pseudo-nitzschia rbc*L. The tree was rooted with *Cylindrotheca* sp. M59080. Black circle indicates boostrap support and bayesian posterior probabilities on >70% and 95%, respectively; gray circle indicates boostrap support below 70% and bayesian posterior probabilities on 95%; gray diamond indicates boostrap support on 70% and bayesian posterior probabilities below 95%. * indicate the species belonging to the *P. pseudodelicatissima* complex.

vata. One HCBC is present in helix I (G-U ↔ A-U) and another in helix III (G-U↔U-A). Four SNPs were also found in helix II (A:U ↔ U U), helix III (U:G ↔ U U and U:G ↔ U C), and helix IV (A:U ↔ U U for *P. granii* and A-U ↔ C U for *P. subcurvata*). Two nucleotide insertions (GA) were found for both *P. granii* and *P. subcurvata* with respect to *P. arctica* on helix III (Fig. 4) and such insertions changed the folding of the tip of helix III. *P. granii* and *P. subcurvata* only differed by a base change in a loop of helix IV (U U↔C U) (Fig. 4).

DISCUSSION

Morphologically, *P. arctica* belongs to the *P. pseudodelicatissima* complex including species having lanceolate to linear narrow valves (transapical axis less than 3.0 μm), uniseriate striae and a central larger interspace. According to this definition, the complex comprises 17 species, *P. arctica*, *P. abrensis* Pérez-Aicua and Orive, *P. batesiana* H.C. Lim, S.T. Teng, C.P. Leaw, and P.T. Lim, *P. caciantha*, *P. calliantha*, *P. circumpora* H.C. Lim, C.P. Leaw, and P.T. Lim, *P. cuspidata*, *P. fryxelliana* Lundholm, *P. fukuyoi* H.C. Lim, S.T. Teng, C.P. Leaw, and P.T. Lim, *P. hasleana*, *P. inflatula* (Hasle) Hasle, *P. kodamae* S.T. Teng, H.C. Lim, C.P. Leaw, and P.T. Lim, *P. lineola* (Cleve) Hasle, *P. lundholmiae* H.C. Lim, S.T. Teng, C.P. Leaw, and P.T. Lim, *P. mannii*, *P. plurisecta* Orive and Pérez-Aicua and *P. pseudodelicatissima* (Lundholm et al. 2003, 2012, Amato et al. 2007, Amato and Montresor 2008, Lim et al. 2012, 2013, Orive et al. 2013, Teng et al. 2014). The shape of the cells is very similar among species and size ranges often overlap. A comparison of cell length is affected by the lack of knowledge of the maximum cell size for most species. Species identification is not possible using LM, since it is based on a combination of fine ultrastructural differences, i.e., number of poroid sectors, density of fibulae, striae and band striae, and structure of the valvocopula, which require the use of electron microscopy. Molecular analyses are often required to further support the morphological species identification.

TABLE 3. Net average nucleotide distance among *P. arctica*, *P. granii*, *P. subcurvata*, and *P. fryxelliana*.

ITS/ITS2 LSU/*rbc*L	*P. arctica*	*P. granii*	*P. subcurvata*
P. granii	0.019/0.032		
	n.a./n.a.		
P. subcurvata	0.019/0.024	0.007/0.008	
	0.012/0.034	n.a./n.a.	
P. fryxelliana	0.133/0.206	0.143/0.205	0.141/0.205
	0.024/0.041	n.a./n.a.	0.030/0.060

n.a., information not available.

The recognition of *P. arctica* as a new species is supported by molecular data, as *P. arctica* shares a very similar ultrastructure with at least one other species in the complex, namely *P. fryxelliana*. Besides having a comparable number of interstriae (33–39 in *P. arctica* and 34–40 in *P. fryxelliana*), fibulae (17–24 and 17–25, respectively), poroid density (4–6 and 5–7 in 1 μm, respectively) and band striae (41–48 and 41–50, respectively), the two species share a remarkable and peculiar variability in poroid structure. In both species, the number of sectors in the poroids can vary from 1 to 5 even in the same stria. In addition, some striae are simply composed of very lightly silicified poroid hymen without any perforations.

Within the complex, *P. arctica* shows also morphological similarities with *P. abrensis*, *P. hasleana*, *P. mannii*, and *P. plurisecta*. However, *P. abrensis* can be differentiated by having a lower density of band interstriae (36–38 vs. 41–48), and *P. hasleana* a lower density of fibulae (13–20 vs. 17–24). In addition, *P. hasleana*, *P. mannii* and especially *P. plurisecta* have a higher number of sectors in poroids than *P. arctica* (2–6, 2–7 and 3–10 respectively vs. 0–5).

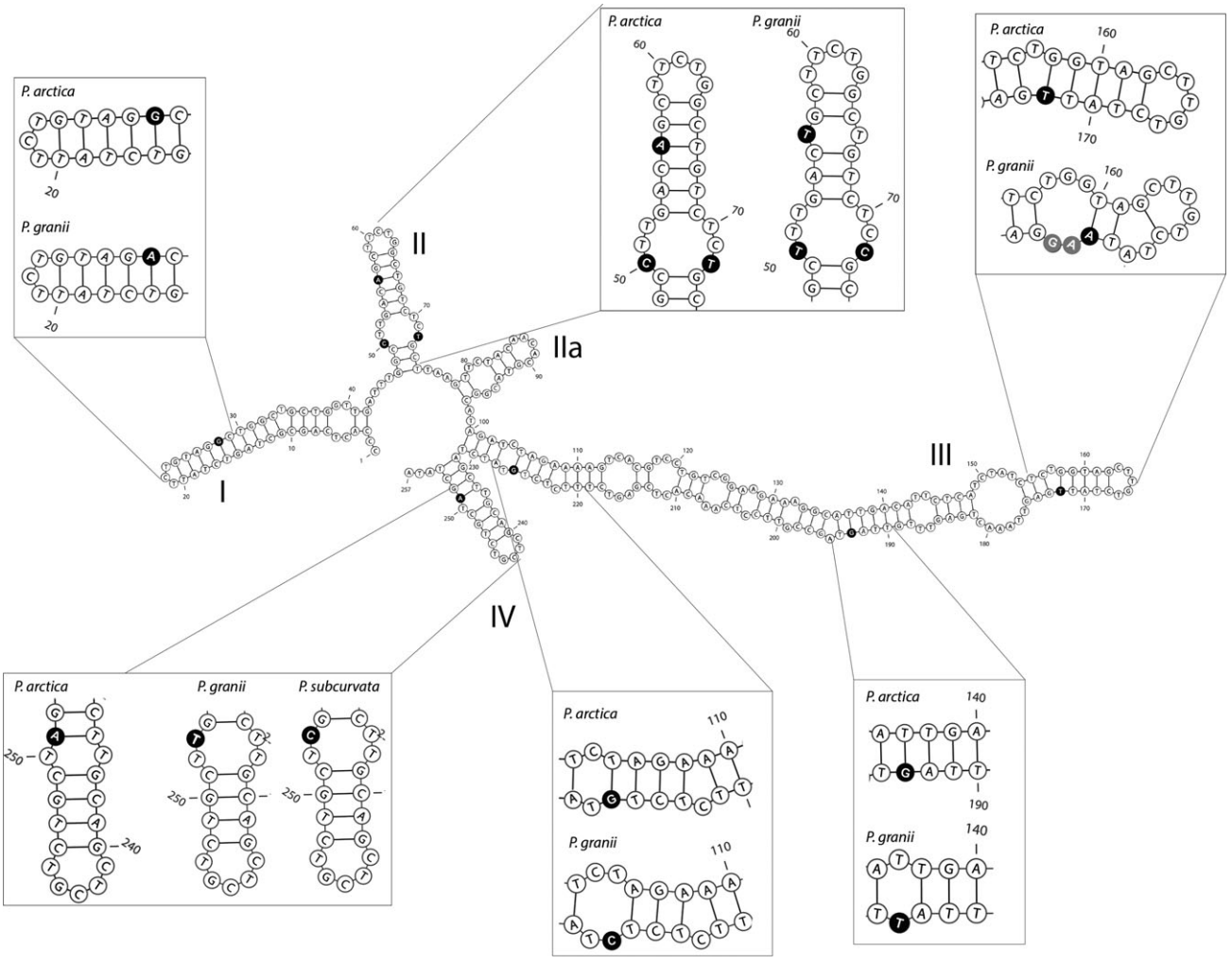

FIG. 4. ITS2 secondary structure of the holotype strain RC2005 for *Pseudo-nitzschia arctica*. Helices are named according to Amato et al. (2007) (roman numbers). The boxes indicate the structural variations found in *P. arctica* with respect to *P. granii* and *P. subcurvata*. Please note that the ITS2 from *P. granii* and *P. subcurvata* differ only by one nucleotide located on the helix IV, whereas it is identical for the rest of the ITS-2 sequence. Nucleotides which differ between *P. arctica* and the other two species are marked with black background, whereas insertions are noted with gray background.

P. batesiana, *P. caciantha*, *P. circumpora*, *P. fukuyoi*, *P. kodamae*, and *P. lundholmiae* have a lower density of fibulae and interstriae than *P. arctica* (see Table 2). In addition, *P. caciantha*, *P. circumpora*, and *P. kodamae* are slightly wider and *P. fukuyoi* is slightly narrower than *P. arctica* (2.2–3.5, 2.2–2.7, 2.1–3.3 and 1.5–1.9 μm, respectively vs. 1.6–2.5 μm). *P. lundholmiae*, moreover, has the poroid hymen generally divided into 1–2 sectors and a lower density of band striae. *P. circumpora* is characterized by a distinctive pore arrangement in the poroids, with the fine pores in each perforation sector arranged in circles, and the presence of rare biseriate striae together with dominant uniseriate striae.

Pseudo-nitzschia arctica can easily be differentiated from *P. cuspidata*, *P. inflatula* and *P. pseudodelicatissima* because the 3 latter species have poroids divided into only two sectors whereas the poroids from *P. arctica* consist in a variable number of sectors (0–5). Moreover *P. cuspidata* and *P. pseudodelicatissima* have a higher density of interstriae than *P. arctica* (35–44 and 36–43 vs. 33–39). *P. pseudodelicatissima* tends also to be narrower than *P. arctica* (0.9–1.6 μm vs. 1.6–2.5 μm).

Pseudo-nitzschia arctica is well distinguishable from *P. lineola* which has the lowest density of fibulae, interstriae and band striae among the species belonging to the complex (10.5–15.5, 22–31, 22–34, respectively). Moreover, *P. lineola* has a slightly atypical stria ultrastructure, having simple poroids organized in 1–2 rows, whereas all the other species have more complex poroids which are always arranged in a single row.

Interestingly, *P. arctica* is morphologically very different from the phylogenetically closely related species, *P. granii* and *P. subcurvata*. The two latter species lack the central large interspace and therefore do not even belong to the *P. pseudodelicatissima* complex. In addition, *P. arctica* has fewer interstriae (33–39 in *P. arctica*, 44–55 in *P. granii*, and 43–55 in *P. subcurvata*) and more fibulae (17–24, 12–20, and 12–22, respectively) than *P. granii* and *P. subcurvata*.

Pseudo-nitzschia granii and *P. subcurvata* are ultrastructurally very similar to each other and are only differentiated by a different cell shape, which is however different from the species belonging to the *P. pseudodelicatissima* complex. *P. granii* has a spindle shaped valve and rounded apices (Hasle and Syvertsen 1997, Marchetti et al. 2008). *Pseudo-nitzschia subcurvata* has a typical curved valve outline with a dilated middle part, one side of the valve straight or slightly concave and the other side convex (Hasle and Syvertsen 1997, Almandoz et al. 2008).

Despite being phylogenetically close to *P. granii* and *P. subcurvata*, *P. arctica* can be considered a distinct genetic unit, as shown by LSU, ITS, *rbc*L phylogenies and supported by the genetic divergence data (Figs. 2, 3, S1 and S2; Table 3). In particular, *rbc*L phylogeny indicates that *P. arctica* and *P. granii* are two different species. *Rbc*L was proven to be more efficient than LSU in discriminating diatom species and the last 738 bp of the *rbc*L gene have been proposed for diatom barcoding (Hamsher et al. 2011). In comparison to a nuclear-encoded marker like ITS, *rbc*L can be more easily amplified, sequenced and aligned. In addition, being a photosynthetic region, it is unlikely to amplify heterotrophic contaminant DNA (MacGillivary and Kaczmarska 2011). The *rbc*L gene has been previously used for the genus *Pseudo-nitzschia*. This gene seems to have a high taxonomic resolution since it can discriminate between closely related taxa such as *P. pungens* var. *pungens* and *P. pungens* var. *cingulata* (Casteleyn et al. 2009). However, the resolutive power of a shorter fragment of the *rbc*L seems to be insufficient for *Pseudo-nitzschia* barcoding (MacGillivary and Kaczmarska 2011). The extent of the taxonomic resolution of the full *rbc*L for the genus *Pseudo-nitzschia* varies according to the species investigated and can be either higher or lower than that of the ITS (Amato et al. 2007). Our data seem to confirm the phylogenetic and taxonomic value of *rbc*L within the genus *Pseudo-nitzschia*, but the efficacy of this marker needs to be assessed based on a larger number of species.

The recognition of *P. arctica* as a separate species is also supported by the analysis of the secondary structure of the ITS2. The presence of CBCs or HCBCs can be used to infer the existence of reproductive isolation in congeneric species (Behnke et al. 2004, Vanormelingen et al. 2007, Coleman 2009). This approach has been largely used in the delineation of *Pseudo-nitzschia* species (e.g., Amato et al. 2007, Casteleyn et al. 2008, Kaczmarska et al. 2008, Lundholm et al. 2012, Lim et al. 2013, Orive et al. 2013, Teng et al. 2015). The analysis of the secondary structure of the ITS2 of all our strains of *P. arctica* shows 2 HCBCs and 2 nucleotide deletions compared to *P. granii* and *P. subcurvata*. These differences, especially the HCBC in the helix III of the ITS2 (Fig. 4), suggest reproductive isolation between *P. arctica* and its two sister species. Although it has been noticed that the presence of CBCs is significantly correlated with mating incompatibility (Coleman 2000, 2005), post-zygotic incompatibility was already observed within the genus *Pseudo-nitzschia* between two species differing only by HCBCs. *P. calliantha* and *P. mannii*, which showed just two HCBCs in helix I and two in helix III, were able to mate but not to form viable auxospores, indicating that a speciation process is in progress due to post-zygotic sexual barriers (Amato et al. 2007, Amato and Montresor 2008).

The morphological and genetic similarity between *P. granii* and *P. subcurvata*, including the presence of a single base change in a loop on helix IV, is intriguing. Strains from the same species can have HCBCs in the helix IV as found in *P. sabit* S.T. Teng, H.C. Lim, P.T. Lim, and C.P. Leaw (Teng et al. 2015), and in general genotypes sharing 100%

identity in the helix II and helix III are considered to belong to the same species. Further investigations, including mating experiments, are required in order to assess whether *P. granii* and *P. subcurvata* are separate species or different genotypes of a single bipolar species.

Despite their morphological similarity, *P. fryxelliana* and *P. arctica* appear in distant positions in all phylogenetic trees. Moreover, the genetic distance between the two species, based on ITS (ITS: 0.133, ITS2: 0.203), is larger than the distance observed between other cryptic, e.g., *P. delicatissima* and *P. arenysensis* (ITS2: 0.1) (Quijano-Scheggia et al. 2009), or pseudo-cryptic species, e.g., *P. delicatissima* and *P. decipiens* (ITS: 0.075–0.090) (Lundholm et al. 2006).

The description of *P. arctica*, which is morphologically similar to *P. fryxelliana*, represents another case of a cryptic species within the *P. pseudodelicatissima* complex. Cryptic diversity has been unveiled in several planktonic and benthic, freshwater and marine microalgal genera, including *Skeletonema* (Sarno et al. 2005, 2007) and *Cyclotella* (Beszteri et al. 2007, Evans et al. 2008). Within the *Pseudo-nitzschia* complex, crypticity has already been shown to exist between *P. pseudodelicatissima* and *P. cuspidata*. The two species share identical ultrastructure and only show slight differences in the valve shape, with the former being linear and the latter lanceolate, which become unclear after repetitive vegetative divisions and the resulting reduction in valve length (Lundholm et al. 2003, 2012). However, the distinction between the two species remains unresolved using LSU rRNA (Amato et al. 2007, Lim et al. 2012, this study) and only partially resolved by ITS analyses (Lundholm et al. 2003, 2006, 2012, Lim et al. 2013, Orive et al. 2013). Only the incorporation of the ITS2 secondary structure in the phylogenetic reconstruction allowed to the separation of the *P. cuspidata* strain Tenerife8 from the *P. pseudodelicatissima* clade (Lim et al. 2013). Similarly, within the *P. delicatissima* complex, *P. delicatissima* and *P. arenysensis* are distinguishable only by molecular evidences (Quijano-Scheggia et al. 2009). In both cases, differently from what observed in *P. arctica* and *P. fryxelliana*, the cryptic species are phylogenetically closely related.

All these findings point out that rates of morphological differentiation, molecular evolution and speciation are incongruent for some *Pseudo-nitzschia* species, as already demonstrated in other planktonic organisms (Lee and Frost 2002, Logares et al. 2007, André et al. 2013).

A direct consequence of the discordant paces of morphological and molecular evolution is the resulting lack of phylogenetic value for some of the taxonomic characters so far considered important for separating *Pseudo-nitzschia* species. The absence/presence of a larger central interspace, i.e., raphe entire or disconnected by a central siliceous nodule, was traditionally considered an important character for species identification in *Pseudo-nitzschia* (Hasle 1965). Initial molecular analyses suggested this feature could have phylogenetic meaning (Orsini et al. 2002), but this hypothesis has been disproven (Lim et al. 2013) and is further challenged in this study. Similarly, the two morphological features used to circumscribe species belonging to the *P. pseudodelicatissima* complex, i.e., presence of uniseriate striae and poroids divided into sectors, have been demonstrated to be phylogenetically uninformative since the first species descriptions (Lundholm et al. 2002, 2012, Lim et al. 2013). Here, we confirm that the *P. pseudodelicatissima* complex is not monophyletic (Figs. 2, 3, Figs. S1 and S2) and that the morphological characters used to discriminate species in the complex are not phylogenetically meaningful, confirming similar speculations for other diatoms, as for example the *Cyclotella meneghiniana* complex (Beszteri et al. 2007, Evans et al. 2008).

The fact that the intraspecific variability in certain morphological traits is difficult to assess limits the use of diagnostic characters for species delimitation. In *P. arctica*, similarly to what observed in *P. fryxelliana* and *P. hasleana* (Lundholm et al. 2012), the ultrastructure of poroids, i.e., the number and size of sectors in the poroids, has been shown to vary among valves of a clonal culture and even among the poroids within a single stria. Only a few studies have focused on frustule ultrastructure plasticity in *Pseudo-nitzschia* species and effect of the environmental factors on morphological characters (Falasco et al. 2009). For example, temperature affects the number of rows of poroids in *P. multiseries* (Lewis et al. 1993) and the number of rows and the density of poroids in *P. seriata* (Hansen et al. 2011). Similarly, salinity affects the length of the intercellular processes in *S. costatum* (Greville) Cleve and *S. subsalsum* (Cleve) Bethge (Balzano et al. 2011) and plays a significant role in the morphological plasticity of the frustule of *Thalassiosira punctigera* (Castracane) Hasle and *T. weissflogii* (Grunow) G. A. Fryxell and Hasle (Vrieling et al. 2007), and *Cocconeis placentula* Ehrenberg and *C. pinnata* W. Gregory ex Greville (Leterme et al. 2013), with main effects on pore size. The latter observations question the validity of the use of the ultrastructure of poroids for species discrimination and stress the importance of the assessment of the morphology based on environmental samples as culture conditions might induce morphological changes. In this study, *P. arctica* morphology has been described based on culture material. Only slight variations in the number of sectors of the poroids and in the level of silification/perforation of the valvocopula have been observed among the six strains analyzed, which have been grown in different culture conditions and media (one strain has been kept in culture since 1989). Nevertheless, the main morphological features used to define *Pseudo-nitzschia* species (i.e. presence of the central larger interspace, number of striae and fibulae, poroids

density) did not significantly vary among the different strains.

Production of domoic acid. Neither of the strains tested positive in any of the tests for production of DA. Negative Elisa test assays do not exclude the possibility of production DA in very low concentrations or under different physiological conditions. The tests of strain P2F2 was, however, performed using LC-MS/MS and induction of DA was attempted both by exposing the strain to silica depletion and grazing by *Calanus* copepods. Silica depletion has previously been shown to increase DA production in several *Pseudo-nitzschia* species (Bates et al. 1998, Fehling et al. 2004), and copepod grazing has been shown to induce DA production in at least two other Arctic *Pseudo-nitzschia* species, *P. seriata* and *P. obtusa* (Hardardotir et al. 2015, Tammilehto et al. 2015). We thus assume that *P. arctica* is nontoxic, although we cannot exclude that other strains can be toxic.

Biogeography. Strains of *P. arctica* analyzed in this study were collected at three distant localities in the Arctic, i.e., the Beaufort Sea, the West Greenland and the Northwest Territories, in different years and in two different seasons (spring and summer). The ITS sequence available in GenBank and identical to *P. arctica* named *P.* cf. *granii* CCMP2093 was isolated from Nunavut, Canada in 1998. These findings question the validity of the *Pseudo-nitzschia* reports from the Canadian Basin based on LM, especially those referring to *P. delicatissima* and *P. pseudodelicatissima* (Horner and Schrader 1982, Booth and Horner 1997, Różańska et al. 2008, Sukhanova et al. 2009), with whom *P. arctica* can be easily confused using LM. Our results suggest that *P. arctica* has a distribution confined to the northern polar area, possibly representing one of the endemic components of the Arctic diatom flora (Balzano et al. pers. obs.). The existence of cold-adapted, geographically restricted ecotypes has been suggested for other Arctic phytoplankton taxa such as the diatom *Chaetoceros neogracilis* (Schütt) VanLandingham, and the Arctic ecotype of the cosmopolitan polyphyletic green alga, *Micromonas pusilla* (Butcher) Manton and Parke, the two autotrophic protists identified as Arctic phylotypes based on their 18S rRNA gene sequence (Lovejoy et al. 2007, Lovejoy and Potvin 2011). Within the genus *Pseudo-nitzschia*, other species appear to be restricted to polar/subpolar waters, i.e., *P. granii* and *P. obtusa* for the Northern area and *P. turgiduloides*, *P. subcurvata*, and *P. prolongatoides* for the Southern area. *P. seriata* shows a wider latitudinal distribution, still circumscribed to the northern hemisphere, being recorded from temperate as well as Arctic regions of the North Atlantic (Hasle and Lundholm 2005). The doubtful report of specimens of *P. seriata* with an atypical stria ultrastructure from the Beagle Channel of Argentina requires further investigation, as pointed out by the authors themselves (Almandoz et al. 2009). Similarly, the unexpected finding of specimens attributed to *P.* cf. *subcurvata* along the Mexican coast of the Gulf of Mexico (Aké-Castillo and Okolodkov 2009) has been recently explained by the description of a new species, *P. sabit*, from plankton samples collected from the Malacca Strait, Malaysia, and the Pacific coast of Mexico (Teng et al. 2015).

A limited number of *Pseudo-nitzschia* species seems to have restricted distribution in nonpolar areas (Lelong et al. 2012). However, assessment of the distributional patterns of cryptic and/or recently described *Pseudo-nitzschia* species will require the use of combined morphological and molecular analyses on material collected in different study areas, including the tropical regions, which are characterized by a high species diversity (Lim et al. 2012, 2013, Teng et al. 2014). Based on the available information, a worldwide distribution seems to be common to most of *Pseudo-nitzschia* species. Cosmopolitism, which was tentatively proposed for most DA-producing taxa (Hasle 2002), has been confirmed for many species after the introduction of molecular approaches in *Pseudo-nitzschia* identification (Lelong et al. 2012). Notably, the use of more variable molecular markers can reveal biogeographic patterns within cosmopolitan species, at the intraspecific level. Distinct distribution patterns characterize the three ITS clades of *P. pungens* which correspond to the morphological varieties *P. pungens* var. *pungens*, *P. pungens* var. *cingulata* and *P. pungens* var. *aveirensis* (Casteleyn et al. 2008, 2009, Churro et al. 2009, Lim et al. 2014). Microsatellite analyses showed that *P. pungens* var. *pungens* has a significant geographic genetic structuring with very restricted gene flow between the different geographic populations (Casteleyn et al. 2010). In *P. pungens*, different physiological features are correlated with morphological and genetic intraspecific differentiation (Kim et al. 2015).

Our observations reinforce the idea of the existence of noncosmopolitan *Pseudo-nitzschia* species, as already suggested by the distribution patterns of other cold-water species.

The incongruity shown here between taxonomy based on morphological characters and molecular phylogeny complicate the study of the genus *Pseudo-nitzschia* but makes *Pseudo-nitzschia* a genus suitable to address interesting questions on speciation and evolution in diatoms.

We are grateful to F. Iamunno and R. Graziano (Electron Microscopy Service, SZN) for EM support, and A. Amato for his valuable suggestions. The study was supported by the EU projects ASSEMBLE-FP7-INFRA-2008-227799 (grant for IP), the Italian RITMARE flagship Project, funded by MIUR under the NRP 2011-2013, approved by the CIPE Resolution 2/2011 of 23.03.2011 (grant for MVR) and MaCuMBA (FP7-KBBE-2012-6-311975).

Aké-Castillo, J. A. & Okolodkov, J. B. 2009. *Pseudo-nitzschia subcurvata* (Bacillariophyceae) in the Gulf of Mexico? *Harmful Algae News* 40:6–7.

Almandoz, G. O., Ferreyra, G. A., Schloss, I. R., Dogliotti, A. I., Rupolo, V., Paparazzo, F. E., Esteves, J. L. & Ferrario, M. E. 2008. Distribution and ecology of *Pseudo-nitzschia* species (Bacillariophyceae) in surface waters of the Weddell Sea (Antarctica). *Polar Biol.* 31:429–42.

Almandoz, G. O., Hernando, M. & Ferrario, M. E. 2009. SEM observations of *Pseudo-nitzschia* from Beagle Channel: *P. seriata* in the southern hemisphere? *Harmful Algae News* 39:6–7.

Amato, A., Kooistra, W. H. C. F., Levialdi Ghiron, J. H., Mann, D. G., Pröschold, T. & Montresor, M. 2007. Reproductive isolation among sympatric cryptic species in marine diatoms. *Protist* 158:193–207.

Amato, A. & Montresor, M. 2008. Morphology, phylogeny, and sexual cycle of *Pseudo-nitzschia mannii* sp. nov. (Bacillariophyceae): a pseudo-cryptic species within the *P. pseudodelicatissima* complex. *Phycologia* 47:487–97.

André, A., Weiner, A., Quillévéré, F., Aurahs, R., Morard, R., Douady, C. J., de Garidel-Thoron, T., Escarguel, G., de Vargas, C. & Kucera, M. 2013. The cryptic and the apparent reversed: lack of genetic differentiation within the morphologically diverse plexus of the planktonic foraminifer *Globigerinoides sacculifer*. *Paleobiology* 39:21–39.

Balzano, S., Sarno, D. & Kooistra, W. H. C. F. 2011. Effects of salinity on the growth rate and morphology of ten *Skeletonema* strains. *J. Plankton Res.* 33:937–45.

Balzano, S., Gourvil, P., Siano, R., Chanoine, M., Marie, D., Lessard, S., Sarno, D. & Vaulot, D. 2012a. Diversity of cultured photosynthetic flagellates in the northeast Pacific and Arctic Oceans in summer. *Biogeosciences* 9:4553–71.

Balzano, S., Marie, D., Gourvil, P. & Vaulot, D. 2012b. Composition of the summer photosynthetic pico and nanoplankton communities in the Beaufort Sea assessed by T-RFLP and sequences of the 18S rRNA gene from flowcytometry sorted samples. *ISME J.* 6:1480–98.

Bates, S. S., Bird, C. J., Freitas, A. S. W. D., Foxall, R., Gilgan, M. W., Hanic, L. A., Johnson, J. E. et al. 1989. Pennate diatom *Nitzschia pungens* as the primary source of domoic acid, a toxin in shellfish from eastern Prince Edward Island, Canada. *Can. J. Fish Aquat. Sci.* 46:1203–15.

Bates, S. S., Garrison, D. L. & Horner, R. A. 1998. Bloom dynamics and physiology of domoic acid-producing *Pseudo-nitzschia* species. *In* Anderson, D. M., Cembella, A. D. & Hallegraeff, G. M. [Eds.] *Physiological Ecology of Harmful Algal Blooms.* Springer-Verlag, Heidelberg, pp. 267–92.

Behnke, A., Friedl, T., Chepurnov, V. A. & Mann, D. G. 2004. Reproductive compatibility and rDNA sequence analyses in *Sellaphora pupula* species complex (Bacillariophyta). *J. Phycol.* 40:193–208.

Beszteri, B., John, U. & Medlin, L. K. 2007. An assessment of cryptic genetic diversity within the *Cyclotella meneghiniana* species complex (Bacillariophyta) based on nuclear and plastid genes, and amplified fragment length polymorphisms. *Eur. J. Phycol.* 42:47–60.

Booth, B. C. & Horner, R. A. 1997. Microalgae on the Arctic Ocean Section, 1994: species abundance and biomass. *Deep-Sea Res. II* 44:1607–22.

Casteleyn, G., Chepurnov, V. A., Leliaert, F., Mann, D. G., Bates, S. S., Lundholm, N., Rhodes, L., Sabbe, K. & Vyverman, W. 2008. *Pseudo-nitzschia pungens* (Bacillariophyceae): a cosmopolitan diatom species? *Harmful Algae* 7:241–57.

Casteleyn, G., Evans, K. M., Backeljau, T., D'hondt, S., Chepurnov, V. A., Sabbe, K. & Vyverman, W. 2009. Lack of population genetic structuring in the marine planktonic diatom *Pseudo-nitzschia pungens* (Bacillariophyceae) in a heterogeneous area in the Southern Bight of the North Sea. *Mar. Biol.* 156:1149–58.

Casteleyn, G., Leliaert, F., Backeljau, T., Debeer, A. E., Kotaki, Y., Rhodes, L., Lundholm, N., Sabbe, K. & Vyverman, W. 2010. Limits to gene flow in a cosmopolitan marine planktonic diatom. *Proc. Natl. Acad. Sci. USA* 107:12952–7.

Churro, C. I., Carreira, C. C., Rodrigues, F. J., Craveiro, S. C., Calado, A. J., Casteleyn, G. & Lundholm, N. 2009. Diversity and abundance of potentially toxic *Pseudo-nitzschia* Peragallo in Aveiro coastal lagoon, Portugal and description of a new variety, *P. pungens* var. *aveirensis* var. nov. *Diatom Res.* 24:35–62.

Cleve, P. T. 1897. Report of the phyto-expedition of H.M.S. "Research". *Fifteenth Ann. Rep. of the Fish. Board of Scotland* 3:296–304.

Coleman, A. W. 2000. The significance of a coincidence between evolutionary landmarks found in mating affinity and a DNA sequence. *Protist* 151:1–9.

Coleman, A. W. 2005. *Paramecium aurelia* revisited. *J. Eukaryot. Microbiol.* 52:68–77.

Coleman, A. W. 2009. Is there a molecular key to the level of "biological species" in eukaryotes? A DNA guide. *Mol. Phylogenet. Evol.* 50:197–203.

Darty, K., Denise, A. & Ponty, Y. 2009. VARNA: interactive drawing and editing of the RNA secondary structure. *Bioinformatics* 25:1974–5.

Degerlund, M. & Eilertsen, H. 2010. Main species characteristics of phytoplankton spring blooms in NE Atlantic and Arctic waters (68–80° N). *Estuar. Coast.* 33:242–69.

Delaney, J. A., Ulrich, R. M. & Paul, J. H. 2011. Detection of the toxic marine diatom *Pseudo-nitzschia multiseries* using the RuBisCO small subunit (*rbc*S) gene in two real-time RNA amplification formats. *Harmful Algae* 11:54–64.

Evans, K. M., Wortley, A. H., Simpson, G. E., Chepurnov, V. A. & Mann, D. G. 2008. A molecular systematic approach to explore diversity within the *Sellaphora pupula* species complex (Bacillariophyta). *J. Phycol.* 44:215–31.

Falasco, E., Bona, F., Badino, G., Hoffmann, L. & Ector, L. 2009. Diatom teratological forms and environmental alterations: a review. *Hydrobiologia* 623:1–35.

Fehling, J., Davidson, K., Bolch, C. & Bates, S. S. 2004. Growth and domoic acid production by *Pseudo-nitzschia seriata* (Bacillariophyceae) under phosphate and silicate limitation. *J. Phycol.* 40:674–83.

Guillard, R. R. L. & Morton, S. L. 2003. Culture methods. *In* Hallegraeff, G. M., Anderson, D. M. & Cembella, A. D. [Eds.] *Manual on Harmful Marine Microalgae.* UNESCO, Paris, France, pp. 77–97.

Hall, T. A. 1999. BioEdit: a user-friendly biological sequence alignment editor and analysis program for Windows 95/98/NT. *Nucl. Acid. Sci.* 41:95–8.

Hamsher, S. E., Evans, K. M., Mann, D. G., Poulícková, A. & Saunders, G. W. 2011. Barcoding diatoms: exploring alternatives to COI-5P. *Protist* 162:405–22.

Hansen, L. R., Soylu, S. I., Kotaki, Y., Moestrup, Ø. & Lundholm, N. 2011. Toxin production and temperature-induced morphological variation of the diatom *Pseudo-nitzschia seriata* from the Arctic. *Harmful Algae* 10:689–96.

Hardardotir, S., Pančić, P., Tammilehto, A., Nielsen, T. G., Krock, B., Møller, E. F. & Lundholm, N. 2015. Dangerous relations in the arctic marine food web – interactions between domoic acid producing *Pseudo-nitzschia* diatoms and *Calanus* copepodites. *Marine Drugs* 13:3809–35.

Hasle, G. R. 1964. *Nitzschia* and *Fragilariopsis* species studied in the light and electron microscopes. I. Some marine species of the groups *Nitzschiella* and *Lanceolatae*. *Skr. Nor. Vidensk-Akad. Oslo I Mat-Naturvidensk. Kl.* 16:1–48.

Hasle, G. R. 1965. *Nitzschia* and *Fragilariopsis* species studied in the light and electron microscopes. II. The group *Pseudo-nitzschia*. *Skr. Nor. Vidensk-Akad. Oslo I Mat-Naturvidensk. Kl.* 18:1–45.

Hasle, G. R. 2002. Are most of the domoic acid-producing species of the diatom genus *Pseudo-nitzschia* cosmopolites? *Harmful Algae* 1:137–46.

Hasle, G. R. & Lundholm, N. 2005. *Pseudo-nitzschia seriata* f. *obtusa* (Bacillariophyceae) raised in rank based on morphological, phylogenetic and distributional data. *Phycologia* 44:608–19.

Hasle, G. R. & Syvertsen, E. E. 1997. Marine diatoms. *In* Tomas, C. R. [Ed.] *Identifying Marine Phytoplankton.* Academic Press, San Diego, California, pp. 5–385.

Horner, R. & Schrader, G. C. 1982. Relative contributions of ice algae, phytoplankton, and benthic microalgae to primary production in nearshore regions of the Beaufort Sea. *Arctic* 35:485–503.

Kaczmarska, I., Reid, C., Martin, J. L. & Moniz, M. B. J. 2008. Morphological, biological, and molecular characteristics of the diatom *Pseudo-nitzschia delicatissima* from the Canadian Maritimes. *Botany* 86:763–72.

Katoh, S. 2013. MAFFT multiple sequence alignment software version 7: improvements in performance and usability. *Mol. Biol. Evol.* 30:772–80.

Keller, M. D., Selvin, R. C., Claus, W. & Guillard, R. R. L. 1987. Media for the culture of oceanic ultraphytoplankton. *J. Phycol.* 23:633–8.

Kim, J. H., Park, B. S., Kim, J. H., Wang, P. & Han, M. S. 2015. Intraspecific diversity and distribution of the cosmopolitan species *Pseudo-nitzschia pungens* (Bacillariophyceae): morphology, genetics, and ecophysiology of the three clades. *J. Phycol.* 51:159–72.

Lee, C. E. & Frost, B. W. 2002. Morphological stasis in the *Eurytemora affinis* species complex (Copepoda: Temoridae). *Hydrobiologia* 480:111–28.

Lelong, A., Hégaret, H., Soudant, P. & Bates, S. S. 2012. *Pseudo-nitzschia* (Bacillariophyceae) species, domoic acid and amnesic shellfish poisoning: revisiting previous paradigms. *Phycologia* 51:168–216.

Leterme, S. C., Prime, E., Mitchell, J., Brown, M. H. & Ellis, A. V. 2013. Diatom adaptability to environmental change: a case study of two *Cocconeis* species from high-salinity areas. *Diatom Res.* 28:29–35.

Lewis, N. I., Bates, S. S., McLachlan, J. L. & Smith, J. C. 1993. Temperature effects on growth, domoic acid production, and morphology of the diatom *Nitzschia pungens* f. *multiseries*. *In* Smayda, T. J. & Shimizu, Y. [Eds.] *Toxic Phytoplankton Blooms in the Sea*. Elsevier Sci. Publ. B.V., Amsterdam, the Netherlands, pp. 601–6.

Librado, P. & Rozas, J. 2009. DnaSP v5: a software for comprehensive analysis of DNA polymorphism data. *Bioinformatics* 25:1451–2.

Lim, H. C., Leaw, C. P., Su, S. N. P., Teng, S. T., Usup, G., Mohammad-Noor, N., Lundholm, N., Kotaki, Y. & Lim, P. T. 2012. Morphology and molecular characterization of *Pseudo-nitzschia* (Bacillariophyceae) from Malaysian Borneo, including the new species *Pseudo-nitzschia circumpora* sp. nov. *J. Phycol.* 48:1232–47.

Lim, H. C., Lim, P. T., Teng, S. T. & Bates, S. S. 2014. Genetic structure of *Pseudo-nitzschia pungens* (Bacillariophyceae) populations: implications of a global diversification of the diatom. *Harmful Algae* 37:142–52.

Lim, H. C., Teng, S. T., Leaw, C. P. & Lim, P. T. 2013. Three novel species in the *Pseudo-nitzschia pseudodelicatissima* complex: *P. batesiana* sp. nov., *P. lundholmiae* sp. nov., and *P. fukuyoi* sp. nov. (Bacillariophyceae) from the Strait of Malacca, Malaysia. *J. Phycol.* 49:902–16.

Logares, R., Rengefors, K., Kremp, A., Shalchian-Tabrizi, K., Boltovskoy, A., Tengs, T., Shurtleff, A. & Klaveness, D. 2007. Phenotypically different microalgal morphospecies with identical ribosomal DNA: a case of rapid adaptive evolution? *Microb. Ecol.* 53:549–61.

Lovejoy, C., Legendre, L., Martineau, M.-J., Bâcle, J. & von Quillfeldt, C. H. 2002. Distribution of phytoplankton and other protists in the North Water. *Deep Sea Res. II* 49:5027–47.

Lovejoy, C. & Potvin, M. 2011. Microbial eukaryotic distribution in a dynamic Beaufort Sea and the Arctic Ocean. *J. Plankton Res.* 33:431–44.

Lovejoy, C., Vincent, W. F., Bonilla, S., Roy, S., Martineau, M. J., Terrado, R., Potvin, M., Massana, R. & Pedrós-Alió, C. 2007. Distribution, phylogeny, and growth of cold-adapted picoprasinophytes in arctic seas. *J. Phycol.* 43: 78–89.

Lundholm, N., Bates, S. S., Baugh, K. A., Bill, B. D., Connell, L. B., Léger, C. & Trainer, V. L. 2012. Cryptic and pseudo-cryptic diversity in diatoms–with descriptions of *Pseudo-nitzschia hasleana* sp. nov. and *P. fryxelliana* sp. nov. *J. Phycol.* 48:436–54.

Lundholm, N., Daugbjerg, N. & Moestrup, Ø. 2002. Phylogeny of the Bacillariaceae with emphasis on the genus *Pseudo-nitzschia* (Bacillariophyceae) based on partial LSU rDNA. *Eur. J. Phycol.* 37:115–34.

Lundholm, N., Moestrup, Ø., Hasle, G. R. & Hoef-Emden, K. 2003. A study of the *Pseudo-nitzschia pseudodelicatissima/cuspidata* complex (Bacillariophyceae): what is *P. pseudodelicatissima*? *J. Phycol.* 39:797–813.

Lundholm, N., Moestrup, Ø., Kotaki, Y., Hoef-Emden, K., Scholin, C. & Miller, P. 2006. Inter- and intraspecific variation of the *Pseudo-nitzschia delicatissima* complex (Bacillariophyceae) illustrated by rRNA probes, morphological data and phylogenetic analyses. *J. Phycol.* 42:464–81.

MacGillivary, M. & Kaczmarska, I. 2011. Survey of the efficacy of a short fragment of the *rbc*L gene as a supplemental DNA barcode for diatoms. *J. Euk. Microbiol.* 58:529–36.

Marchetti, A., Lundholm, N., Kotaki, Y., Hubbard, K., Harrison, P. J. & Armbrust, E. V. 2008. Identification and assessment of domoic acid production in oceanic *Pseudo-nitzschia* (Bacillariophyceae) from iron-limited waters in the North-East Subarctic Pacific. *J. Phycol.* 44:650–61.

McDonald, S. M., Sarno, D. & Zingone, A. 2007. Identifying *Pseudo-nitzschia* species in natural samples using genus-specific PCR primers and clone libraries. *Harmful Algae* 6:849–60.

Nei, M. 1987. *Molecular Evolutionary Genetics*. Columbia University Press, New York, 512 pp.

Orive, E., Pérez-Aicua, L., David, H., García-Etxebarria, K., Laza-Martínez, A., Seoane, S. & Miguel, I. 2013. The genus *Pseudo-nitzschia* (Bacillariophyceae) in a temperate estuary with description of two new species: *Pseudo-nitzschia plurisecta* sp. nov. and *Pseudo-nitzschia abrensis* sp. nov. *J. Phycol.* 49:1192–206.

Orsini, L., Sarno, D., Procaccini, G., Poletti, R., Dahlmann, J. & Montresor, M. 2002. Toxic *Pseudo-nitzschia multistriata* (Bacillariophyceae) from the Gulf of Naples: morphology, toxin analysis and phylogenetic relationships with other *Pseudo-nitzschia* species. *Eur. J. Phycol.* 37:247–57.

Poulin, M., Daugbjerg, N., Gradinger, R., Ilyash, L., Ratkova, T. & von Quillfeldt, C. 2011. The pan-Arctic biodiversity of marine pelagic and sea-ice unicellular eukaryotes: a first-attempt assessment. *Mar. Biodiv.* 41:13–28.

Priisholm, K., Moestrup, Ø. & Lundholm, N. 2002. Taxonomic notes on the marine diatom genus *Pseudo-nitzschia* in the Andaman Sea near the island of Phuket, Thailand, with a description of *Pseudo-nitzschia micropora* sp. nov. *Diatom Res.* 17:153–75.

Quijano-Scheggia, S. I., Garcés, E., Lundholm, N., Moestrup, Ø., Andree, K. & Camp, J. 2009. Morphology, physiology, molecular phylogeny and sexual compatibility of the cryptic *Pseudo-nitzschia delicatissima* complex (Bacillariophyta), including the description of *P. arenysensis* sp. nov. *Phycologia* 48:492–509.

von Quillfeldt, C. H. 1997. Distribution of diatoms in the Northeast Polynya, Greenland. *J. Marine Syst.* 10:211–40.

von Quillfeldt, C. H. 2000. Common diatom species in Arctic spring blooms: their distribution and abundance. *Bot. Mar.* 43:499–516.

Ratkova, T. N. & Wassmann, P. 2002. Seasonal variation and spatial distribution of phyto- and protozooplankton in the central Barents Sea. *J. Marine Syst.* 38:47–75.

Ratkova, T. N. & Wassmann, P. 2005. Sea ice algae in the White and Barents seas: compositon and origin. *Polar Res.* 24:95–110.

Ratkova, T. N., Wassmann, P., Verity, P. G. & Andreassen, I. J. 1998. Abundance and biomass of pico-, nano-, and microplankton on a transect across Nordvestbanken, north Norwegian shelf, in 1994. *Sarsia* 84:213–25.

Ronquist, F. & Huelsenbeck, J. P. 2003. MrBayes version 3.0: Bayesian phylogenetic inference under mixed models. *Bioinformatics* 19:1572–4.

Round, F. E., Crawford, R. M. & Mann, D. G. 1990. *The Diatoms. Biology and Morphology of the Genera*. Cambridge University Press, Cambridge, UK, 747 pp.

Różańska, M., Poulin, M. & Michel, G. 2008. Protist entrapment in newly formed sea ice in the Coastal Arctic Ocean. *J. Marine Syst.* 74:887–901.

Ruggiero, M. V., Sarno, D., Barra, L., Kooistra, W. H. C. F., Montresor, M. & Zingone, A. 2015. Diversity and temporal pattern of *Pseudo-nitzschia* species (Bacillariophyceae) through the molecular lens. *Harmful Algae* 42:15–24.

Sarno, D., Kooistra, W. C. H. F., Balzano, S., Hargraves, P. E. & Zingone, A. 2007. Diversity in the genus *Skeletonema* (Bacillariophyceae): III. Phylogenetic position and morphological variability of *Skeletonema costatum* and *Skeletonema grevillei*, with the description of *Skeletonema ardens* sp. nov. *J. Phycol.* 43:156–70.

Sarno, D., Kooistra, W. C. H. F., Medlin, L. K., Percopo, I. & Zingone, A. 2005. Diversity in the genus *Skeletonema* (Bacillariophyceae). II. An assessment of the taxonomy of *S. costatum*-like species, with the description of four new species. *J. Phycol.* 41:151–76.

Scott, F. J. & Thomas, D. P. 2005. Diatoms. *In* Scott, F. J. & Marchant, H. J. [Eds.] *Antarctic Marine Protists.* Australian Biological Resources Study, Australian Antarctic Division, Canberra & Hobart, pp. 13–201.

Sukhanova, I. N., Flint, M. V., Pautova, L. A., Stockwell, D. A., Grebmeier, J. M. & Sergeeva, V. M. 2009. Phytoplankton of the western Arctic in the spring and summer of 2002: structure and seasonal changes. *Deep Sea Res. II* 56:1223–36.

Tammilehto, A., Nielsen, T. G., Krock, B., Møller, E. F. & Lundholm, N. 2012. *Calanus* spp.—Vectors for the biotoxin, domoic acid, in the Arctic marine ecosystem? *Harmful Algae* 20:165–74.

Tammilehto, A., Nielsen, T. G., Krock, B., Møller, E. F. & Lundholm, N. 2015. Induction of domoic acid production in the toxic diatom *Pseudo-nitzschia seriata* by calanoid copepods. *Aquat. Toxicol.* 159:52–61.

Tamura, K., Peterson, D., Peterson, N., Stecher, G., Nei, M. & Kumar, S. 2011. MEGA5: molecular evolutionary genetics analysis using maximum likelihood, evolutionary distance, and maximum parsimony methods. *Mol. Biol. Evol.* 28:2731–9.

Teng, S. T., Lim, H. C., Lim, P. T., Dao, V. H., Bates, S. S. & Leaw, C. P. 2014. *Pseudo-nitzschia kodamae* sp. nov. (Bacillariophyceae), a toxigenic species from the Strait of Malacca. *Malaysia. Harmful Algae* 34:17–28.

Teng, S. T., Lim, P. T., Lim, H. C., Rivera-Vilarelle, M., Quijano-Scheggia, S., Takata, Y., Quilliam, M. A., Wolf, M., Bates, S. S. & Leaw, C. P. 2015. A non-toxigenic but morphologically and phylogenetically distinct new species of *Pseudo-nitzschia*, *P. sabit* sp. nov. (Bacillariophyceae). *J. Phycol.* 51:706–25.

Trainer, V. L., Bates, S. S., Lundholm, N., Thessen, A. E., Cochlan, W. P., Adams, N. G. & Trick, C. G. 2012. *Pseudo-nitzschia* physiological ecology, phylogeny, toxicity, monitoring and impacts on ecosystem health. *Harmful Algae* 14:271–300.

Tuschling, K., Von Juterzenka, K., Okolodkov, Y. & Anoshkin, A. 2000. Composition and distribution of the pelagic and sympagic algal assemblages in the Laptev Sea during autumnal freeze-up. *J. Plankton Res.* 20:843–64.

Vanormelingen, P., Chepurnov, V. A., Mann, D. G., Cousin, S. & Vyverman, W. 2007. Congruence of morphological, reproductive and ITS rDNA sequence data in some Australasian *Eunotia bilunaris* (Bacillariophyta). *Eur. J. Phycol.* 42:61–79.

Vrieling, E. G., Sun, Q., Tian, M., Kooyman, P. J., Gieskes, W. W. C., van Santen, R. A. & Sommerdijk, N. A. J. M. 2007. Salinity-dependent diatom biosilicification implies an important role of external ionic strength. *Proc. Natl. Acad. Sci. USA* 104:10441–6.

Wassmann, P., Ratkova, T. N., Andreassen, I., Vernet, M., Pedersen, G. & Rey, F. 1999. Spring bloom development in the marginal ice zone and the central Barents Sea. *Mar. Ecol.-Evol. Persp.* 20:321–46.

White, T. J., Bruns, T., Lee, S. & Taylor, J. 1990. Amplification and direct sequencing of fungal ribosomal RNA genes for phylogenetics. *In* Innis, M. A., Gelfand, D. H., Sninsky, J. J. & White, T. J. [Eds.] *PCR Protocols.* Academic Press, New York, pp. 315–22.

Wolf, M., Achtziger, M., Schultz, J., Dandekar, T. & Muller, T. 2005. Homology modeling revealed more than 20,000 rRNA internal transcribed spacer 2 (ITS2) secondary structures. *RNA* 11:1616–23.

Zuker, M., Mathews, D. H. & Turner, D. H. 1999. Algorithms and thermodynamics for RNA secondary structure prediction: a practical guide. *In* Barciszewski, J. & Clark, B. F. C. [Eds.] *RNA Biochemistry and Biotechnology.* Springer, Dordrecht, the Netherlands, pp. 11–43.

Supporting Information

Additional Supporting Information may be found in the online version of this article at the publisher's web site:

Figure S1. Phylogenetic tree from ML analysis based on the *Pseudo-nitzschia* D1–D3 LSU rDNA.

Figure S2. Phylogenetic tree from ML analysis based on the *Pseudo-nitzschia* ITS2 rDNA.

Table S1. List of primer pairs used in present study for amplification.

Table S2. List of strains used in the phylogenetic analyses of LSU, ITS, ITS2, and *rbc*L, showing species identity, strain designation, isolation site, and accession numbers.